Acta Microscópica, Vol. 1, Nº 1, May 1992, pp 20-28

Optimization of Electron Optics for Low Voltage Scanning Electron Microscopy

Yumin Jia* and David C Joy**
EM Facility University of Tennessee, Knoxville, TN 37966-0810
*CSIMC Philips EM Service Center, Beijing China
**High Temperature Materials Laboratory, Oak Ridge National Laboratory, Oak Ridge TN 37831. USA.

INTRODUCTION

The resolution of the scanning electron microscope (SEM) depends on the diameter of the incident electron probe, and on the quantity of current this probe contains. These quantities, in turn, are dependent on the nature of the electron source, on the quality of the imaging lenses and, in particular, of the choice of the defining aperture in the probe forming lens which sets the beam convergence angle α. At medium to high beam energies, that is to say above about 10keV, the optimum operating aperture can be found analytically by assuming that diffraction and spherical aberration are the only significant aberrations. At low beam energies, typically below 5 keV, however diffraction effects, and spherical and chromatic aberrations are all of equal significance and a meaningful analytical solution is difficult to produce because the various aberrations contributions to this probe do not all have the same form. In this papaer we describe a Monte Carlo based numerical ray tracing program which provides an accurate geometrical model of the process of probe formation by a lens. We can use this to derive information about the size, shape and current of electron probes under a variety of conditions, and hence find the optimum operating aperture.

METHOD

The method used here is based on the program DOCCALC (Disc of least Confusion Calculation) originally described by Kenway and Cliff [1] which uses geometrical optics to describe the trajectory of an electron through the electron magnetic lens (Fig. 1). In the simplest case of a lens free from aberration all of the rays leaving the object plane would pass through a focus at the image plane. For a real lens with a finite spherical aberration coefficient (C_s) the position at which the electron crosses the axis is ahead of the nominal image plane by the amount ∂z where

$$\partial z = C_s \alpha^2 \quad (1)$$

where α made is the angle made by the electron with the optic axis. Similarly if the lens has a finite chromatic aberration coefficient (C_c) then the electron trajectories cross the optic axis a further distance ∂z ahead of the image plane given by the relation

$$\partial z = C_c \Delta E / E_o \quad (2)$$

where ΔE is the energy spread of the incident electron beam and E_o is the incident beam energy.

For the simplest analysis of an electron optical system it is customary to assume that ΔE and α are constant, and that all of the electrons leave from the point where the object plane cuts the optic axis. While this often makes it possible to obtain an analytical result for the choice of α it is an oversimplification because the angle and energy, and the actual coordinates of the point within the object from which the electron leaves, are independent variables. Thus each electron leaves the object at some arbitrary angle γ to the axis where $0 \leq \gamma \leq \alpha$, has energy $E_o - \Phi$ where $0 \leq \Phi \leq \Delta E$, and leaves from a point x_o, y_o where $(x_o^2 + y_o^2) \leq s_o^2$ where s_o is the radius of the object.

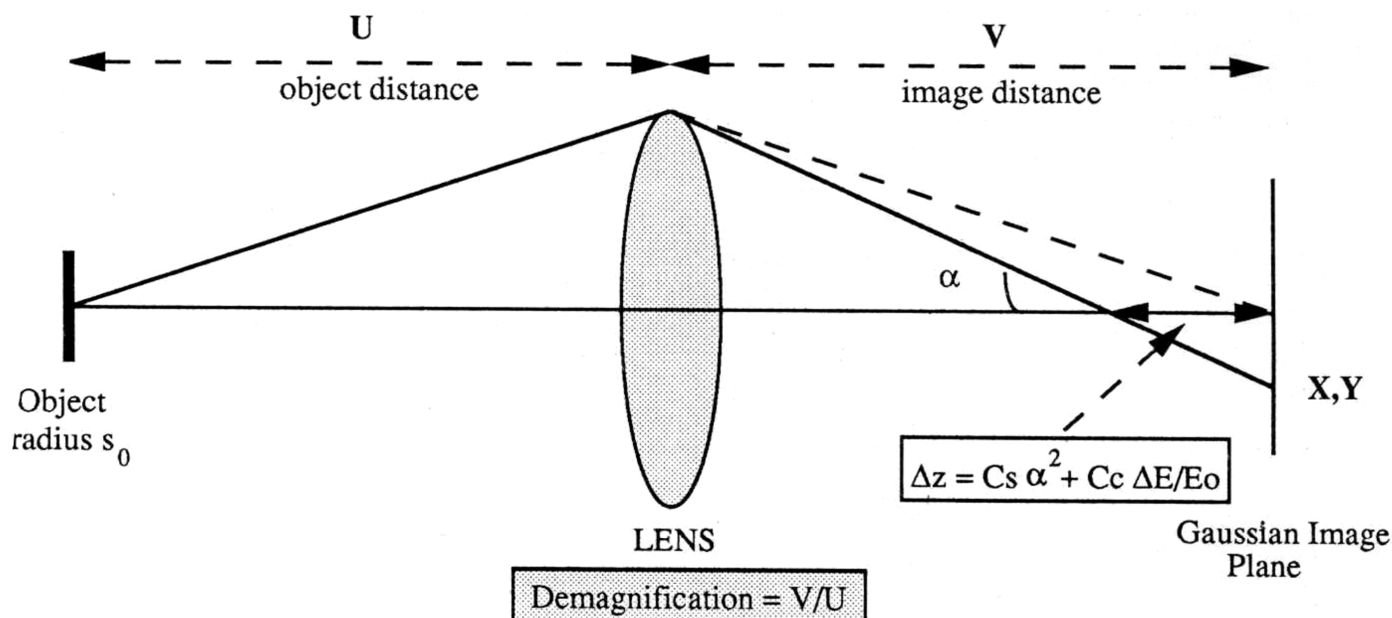

Fig. 1.- Schematic arrangement of optics used in the simulation procedure.

An accurate model of the probe forming process will therefore have to consider both the best possible combination of these variables as well as the worst combination and all posible values in between.

In this program a simple Monte Carlo approach is used to achieve this result. The program takes as input the focal length of the lens, the spherical (C_s) and chromatic (C_c) aberration coefficients of the lens, the demagnification of the lens (DMG), the maximum cone of illumination from the object (α), the diameter of the object(s_o), the energy of the electrons (E_o), the energy spread of the electrons (DelE) and the distance (DEFOCUS) between the actual plane in which the image is to be formed and the Gaussian image plane. The user also selects how many electron trajectories will be run -typically sufficiently good data can be achived with from 2000 to 5000 electrons. For each electron the identical procedure is followed. The electron leaves the object point at some arbitrary azimuthal angle phi where

$$phi=2\pi.RND \quad (3)$$

and RND is an equidistributed random number $0 \leq RND \leq 1$. Its starting radius from the optic axis r_o is given as

$$r_o=s_o\sqrt{-\ln(RND)} \quad (4)$$

where ln is a natural logarithm and the intent is that this function will roughly approximate a Gaussian distribution. The angle ao that the electron makes to the axis as it leaves is

$$a_o=\alpha\sqrt{RND} \quad (5)$$

Equations (3)-(5) completely define the starting trajectory of the electron. Using the conventional geometrical ray equations for a thin lens and the specified focal length and demagnification, the coordinates X,Y of the point where the electron intersects the image plane can then be computed. Because these equations are cumbersome they are not reproduced here, but they can be found in Kenway and Cliff [1]. These landing coordinates are plotted directly on the screen on the computer to give an immediate impression of the form of the probe. The coordinates are also stored in an array for subsequent processing.

After the program has run the desired number of trajectories (a process which on an Apple Macintosh personal computer requires about 3 minutes for 2500 events) the complete set of landing coordinates is converted to a radial distribution by counting the number of trajectories which finish inside an annular ring of specified inner and outer radius. For the type of data shown here the separation of the rings was 4Å, but different electron optical conditions would require different choices. This radial distribution

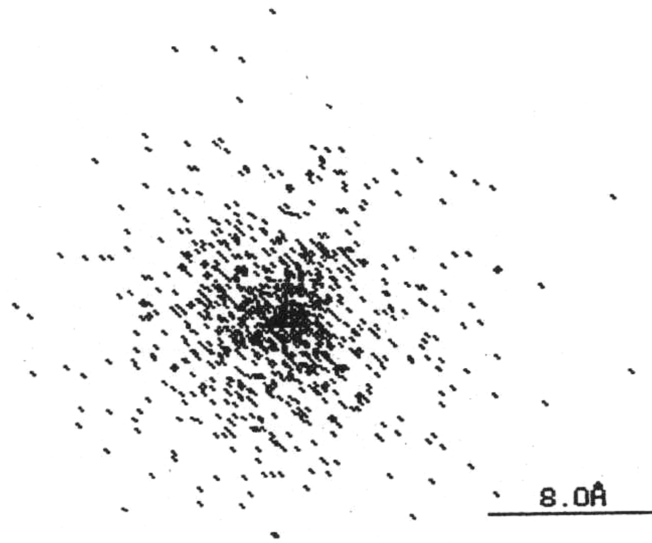

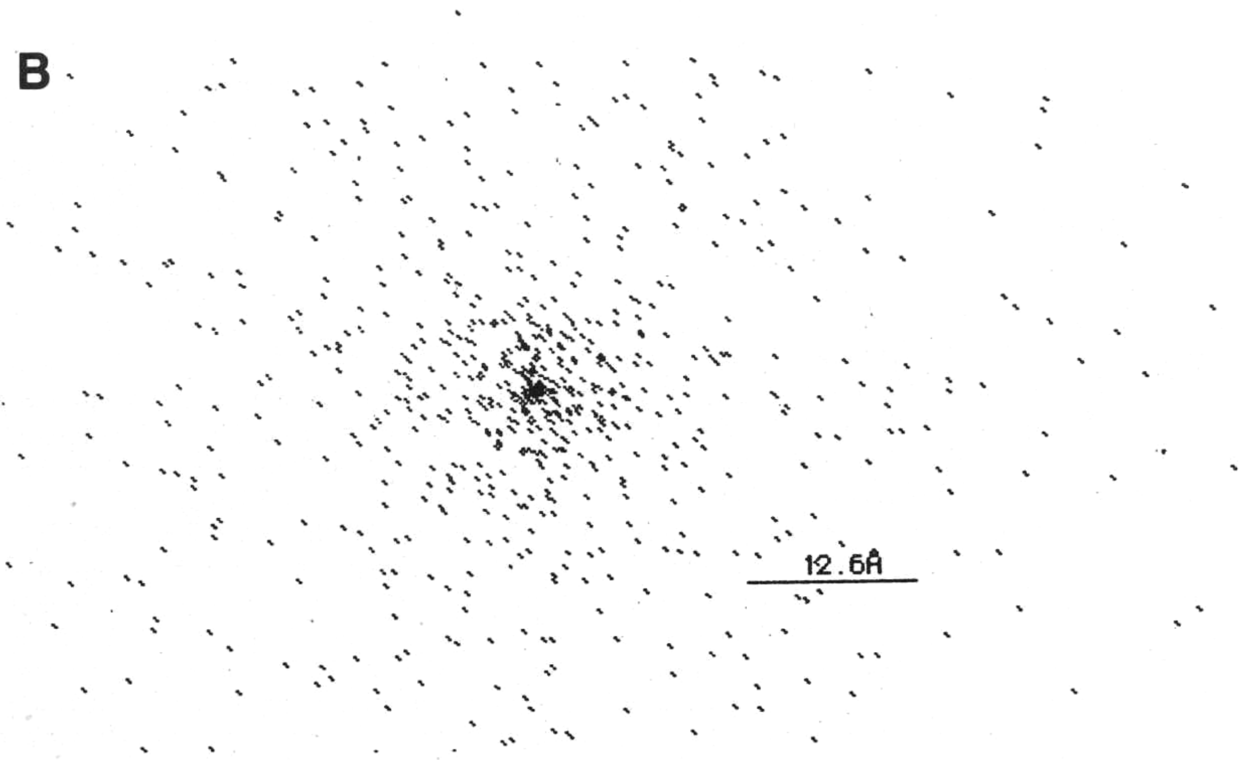

Fig. 2a.- Plot of the landing position of 1000 electrons for a field emission gun operating at 5keV, assumed to have an energy spread of 0.25eV, used with a high resolution immersion type lens for which the focal lenght is 3.6mm, the C_c is 1.9mm and C_c is 2.5mm.
Fig. 2b.- Comparison plot for a conventional tungsten hairpin electron gun at 5keV, assumed to have an energy spread of 3eV, an using a typical 'pinhole' lens with a focal length of 10mm, a C_s of 12 mm and a C_c of 15mm.

$I_o(r)$ is then numerically convoluted with the diffraction profile I_D for a point source,

$$I_D(r) = \text{constant}.\ \frac{2J_1(2\pi\alpha)}{\alpha} \qquad (6)$$

(where J_1 is a Bessel function of the first kind) to give the final radial profile $I_p(r)$. This profile can then be plotted and measured to determine the parameters of interest.

RESULTS

Figures 2(a) and (b) show two examples of how this program allows the electron probe to be visualized. The figures show the landing positions for 1000 electrons for two different SEM configurations, both operating at 5keV beam energy. In figure 2(a) the probe is from a field emission gun (FEG) SEM, assumed to have an energy spread of 0.25eV, and a high resolution immersion type lens for which the focal length is 3.6mm, the C_s is 1.9mm and the C_c is 2.5mm. In figure 2(b) the probe is that formed from a conventional tungsten hairpin electron gun, assumed to have an energy spread of 3eV, and using a typical "pinhole" lens with a focal length of 10mm, a Cs of 12mm and a Cc of 15mm. The differences between the probes is evident from the plot of the electron distribution. For the FEG SEM (Fig. 2a) the probe is tightly confined with the great majority of the current on, or close to, the optic axis. For the thermionic emitter (Fig. 2b) the probe is uniformly distributed over a considerable diameter, with little evidence of a peak of current on the actual axis.

While these two examples represent different extremes of optical performance they demonstrate that the "quality" of an electron probe cannot be described simply by quoting its diameter. Not only is the second probe larger than the first, but the fact that there is no central peak of current and a large, diffuse, skirt of electrons suggests that the images produced in this case will also be low in contrast and harder to focus. In order to quantify such effects it is necessary to use other ways of displaying the data. Figure 3 shows the two alternatives provided by the program. Firstly we can display the actual radial current density profile $I_p(r)$,

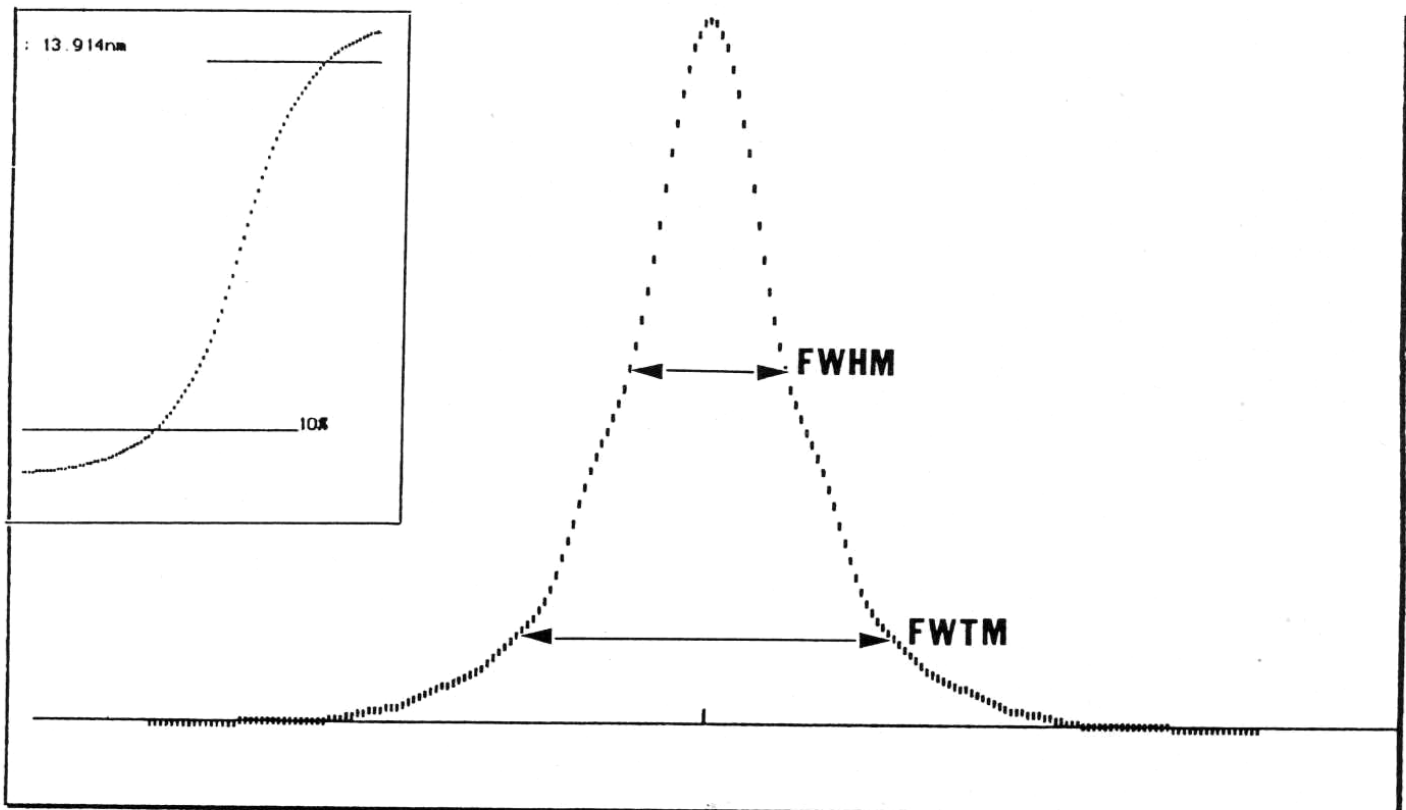

Fig. 3.- Profile, from the data of Fig. 2b showing the normalized radial current distribution in the probe. The inset in the figure shows the corresponding 'rise' profile generated by scanning the radial profile over an edge. The lateral distance between the points representing 10% and 90% of the peak signal level is a convenient measure of the resolution of the probe.

normalized so that

$$\int_0^\infty 2\pi I_p(r) r dr = 1 \qquad (7)$$

The display then indicates the peak current (i.e. the current on the axis) which is a useful measure of how well the optics are performing. If the probe has the ideal Gaussian profile then the peak current is $1/\sqrt{2\pi} \approx 0.4$. A peak value significantly lower than this indicates that the aberrations of the optical system are transferring current from the axis to the skirt of the probe. This clearly implies that the shape of the probe profile is now "non-Gaussian", but whether or not this is reflected in the size of the probe depends on how this quantity is defined. Typically the diameter of the probe is specified as its full width at half maximum height (FWHM), however even if there is a substancial transfer of current from the center of the probe to the skirt then the FWHM value may not change. However the full width at one tenth maximum height (FWTM) is much more sensitive to such variations. For an ideal Gaussian probe the ratio of FWTM/FWHM is about 2, but for a probe with significant skirts this same ratio may be higher. For example for the profile in Fig. 3 the FWHM is 84Å while the FWTM is 224Å, for a ratio of 2.6:1. Thus when considering the electron optical optimization it is not sufficient to minimize the FWHM unless the FWTM and its ratio to the FWHM are also minimized. An alternative definition relies on the experimental "rise-time" technique for measuring probe diameters (e.g Lyman et al [2]) in which the beam is scanned over a sharp edge, and the lateral distance traveled by the beam as the signal rises from 10% to 90% of its maximum value is defined as the probe size, an experiment which can be simulated on the computer by integrating $I_p(r)$ appropiately. This type of measurement is sensitive both to the near axis and off axis shape of the probe and is therefore a useful single number parameter for quantifying the probe size. The inset on Fig. 3 displays the corresponding rise profile for the current profile shown together with the 10% and 90% level markings. The measured "resolution" 10%-90% in this case is 140Å, a figure which lies between the FWHM and FWTM values, indicating its value as a convenient measure of the size.

DISCUSSION

The utility of this approach will be demonstrated by an analysis of the electron optical system of the Hitachi S-900 high resolution SEM for a field emission and a LaB_6 gun. The S-900 has a probe forming lens for which the focal length is 3.6mm, a C_s of 1.9mm and a C_c of 2.5mm. We will assume that for either electron source the lens is run at the same demagnification of x10 and with an effective object source size of 5nm. The FEG is assumed to have an energy spread of 0.15eV while the LaB_6 is taken to have an energy spread of 2eV. In every case the probe profile has been calculated for the Gaussian image plane position. The variables which can be changed in the simulation are thus the incident electron energy and the aperture angle α. For a fixed beam energy the effect of varying α can then be studied to determine the optimum value. Figs 4 and 5 show how the probe diameter-defined here as being the resolution determined from the 10%-90% rise time as in Fig. 3- varies with α for the LaB_6 and FEG emitters at 1.5keV. The peak current value is also plotted in each case to give an indication of how "Gaussian" the beam profile is. For the LaB_6 source the probe size shows a significant minimum for a convergence angle of just about 4m.rads. This corresponds well with the peak in the current plot indicating that, at this aperture value, the best resolution is obtained (i.e the probe size is minimized) precisely because the profile at this condition has the most Gaussian shape. The data for the FEG source is similar, although the aperture angle at which the minimum occurs is about twice that for the LaB_6 gun. The variation of the peak current with aperture size is also less pronounced for the FEG and the value of the peak current is about twice that of the LaB_6 case. These disparities are attributable to the differences in the energy spreads of the two electron sources and hence in the chromatic aberration components of the beam in the two cases. The LaB_6 probe is wider, i.e less Gaussian in shape, because of the effect of chromatic aberration and in order to keep this effect in control it is then necesary to choose a smaller beam convergence angle than would otherwise have been desirable.

The same procedure can be employed at every beam energy to determine an optimum

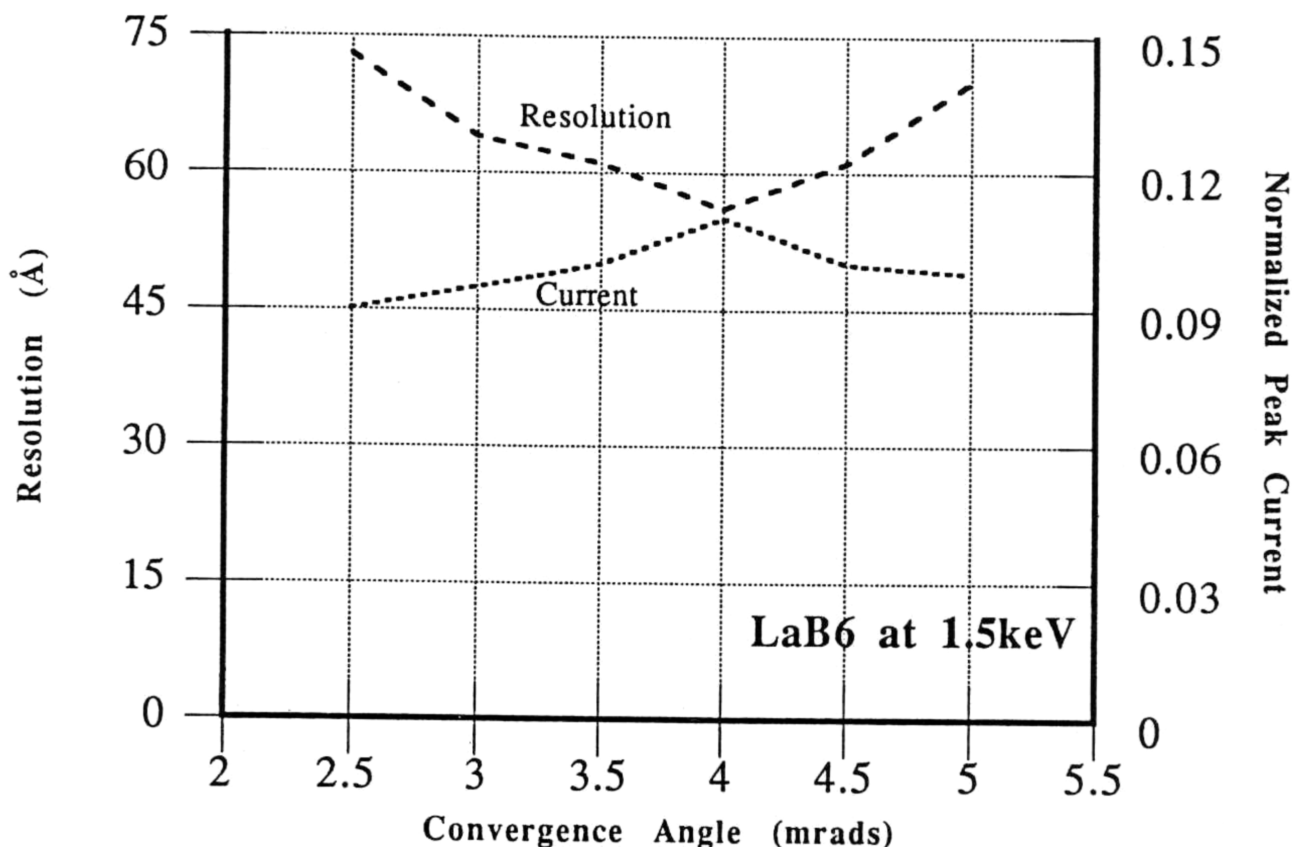

Fig. 4.- Variation of probe resolution and peak axial current as a function of the beam convergence angle for an LaB_6 source at 1.5keV and the Hitachi S-900 lens configuration described in the text.

aperture angle for the two systems, and hence to find the best attainable resolution for the systems. Figure (6) shows how the resolution varies as a function of beam energy for the two cases under the conditions specified above. At high beam energies (>10keV) where the effect of chromatic aberration is negligible the two sources both produce a beam of the same diameter, but as the energy is reduced from 30keV to 500eV the resolution of the LaB_6 beam worsens by about ten times, while that of the FEG source degrades by a factor of about two times. This clearly demonstrates that, even with a state of the art electron lens, for effective low energy scanning electron microscopy a field emission source of low energy spread is essencial in order to obtain good resolution.

The actual value of the optimum aperture angle for the two cases is plotted in Fig. 7. As would be expected, at high beam energies both systems require the same aperture but while the aperture for the FEG actually slightly increases in size as the beam energy is reduced, so helping to minimize the diffraction, the required aperture for the LaB_6 case significantly decreases in order to keep down the chromatic aberration. The graph also shows for comparison a theoretical estimate of the optimum aperture size. The probe size d can be written as

$$d^2=d_o{}^2+d_s{}^2+d_d{}^2 \tag{8}$$

where d_o is the geometric probe size,

$$d_s = 1/2C_s\alpha^3 \text{ and } d_d = \lambda/\alpha$$

and λ is the electron wavelength. If the brightness of the electron source is β then

$$\beta = \frac{4\, I_b}{\pi^2\, d_0^2\, \alpha^2} \tag{9}$$

where I_b is the incident current at the specimen. Substituting equation (8) into equation (9) and differentiating to find the value of α which gives the maximum value of I_b for a given value of d gives [3, 4].

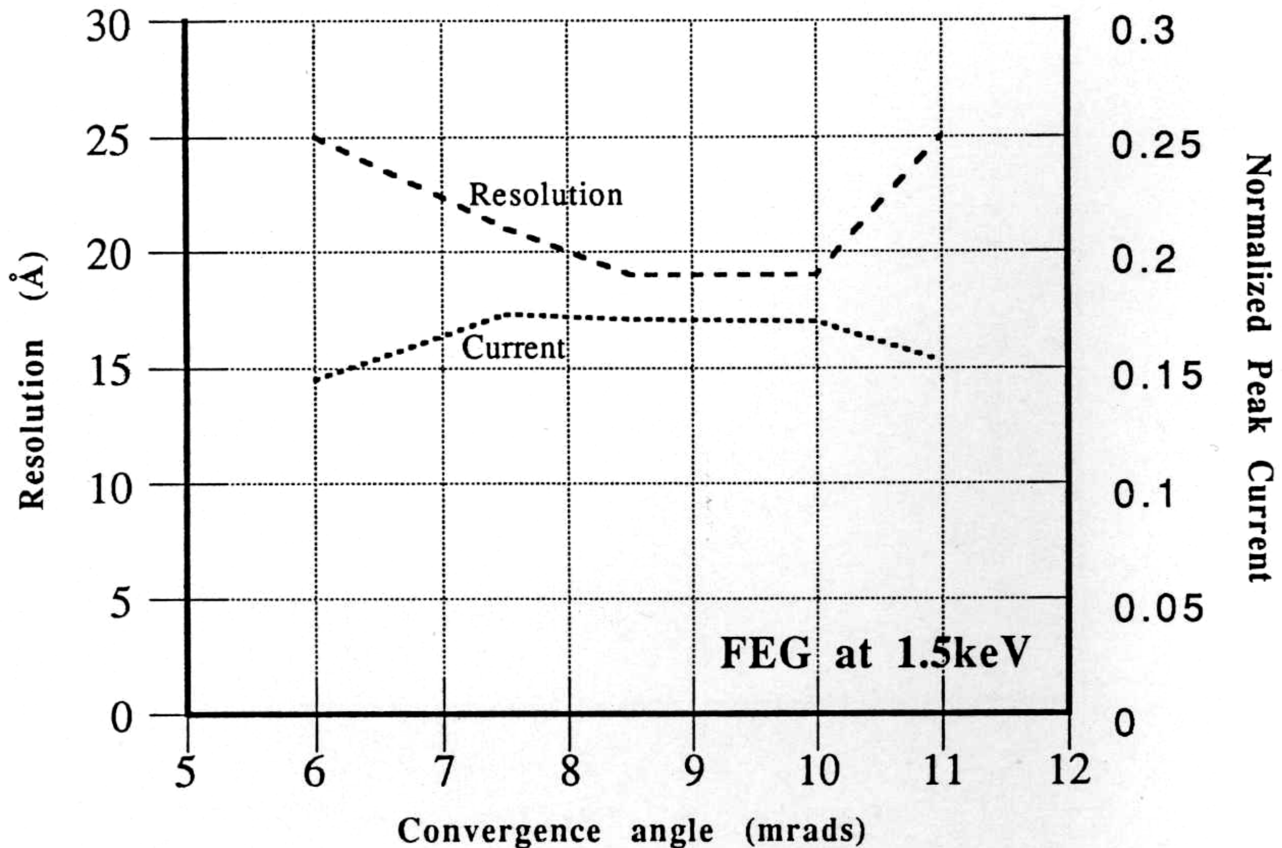

Fig. 5.- Variation of probe resolution and peak axial current as a function of the beam convergence angle for an FEG source at 1.5keV and the S-900 lens configuration described in the text.

$$\alpha = \left(\frac{d}{C_s}\right)^{1/3} \quad \text{and } I_b = \frac{1.88\ \beta\ d^{8/3}}{C_s^{2/3}}$$

The values of α calculated from this expression, using the values of d plotted in Fig. 6, are superimposed on Fig. 7. The predicted values for the FEG have the same general trend and value as those derived from the complete analysis described above, but for the LaB_6 case the trend of the predicted values is opposite to that determined by the simulation and, except at the highest energy values, the values are substantially larger. The relative failure of this often used procedure is due to several factors; firstly the neglect of chromatic aberration, secondly the assumption that terms can be added in quadrature (equation 8) even when the shapes of these profiles are different, and thirdly the assumption that each of the aberration terms is fixed in magnitude rather than distributed over a range of values.

Finally Fig. 8 plots the variation of the normalized peak current as a function of beam energy for this set of data. As discussed above this effectively displays how Gaussian in shape the probe actually is. At high beam energies both electron sources produce probes of good shape, but as the energy is reduced the LaB_6 probe rapidly degrades in shape until at 1keV it has less than a quarter as much of its current on axis as expected. Conversely the FEG probe also worsens in shape but at a much lower rate, maintaining a good level of performance at most energies.

CONCLUSIONS

The computer simulation ray-tracing procedure described here provides a general, and accurate way to study the process of probe forming in a SEM and to study how the choice of electron-optical conditions affects the quality of the beam. In all except the limiting case of operation

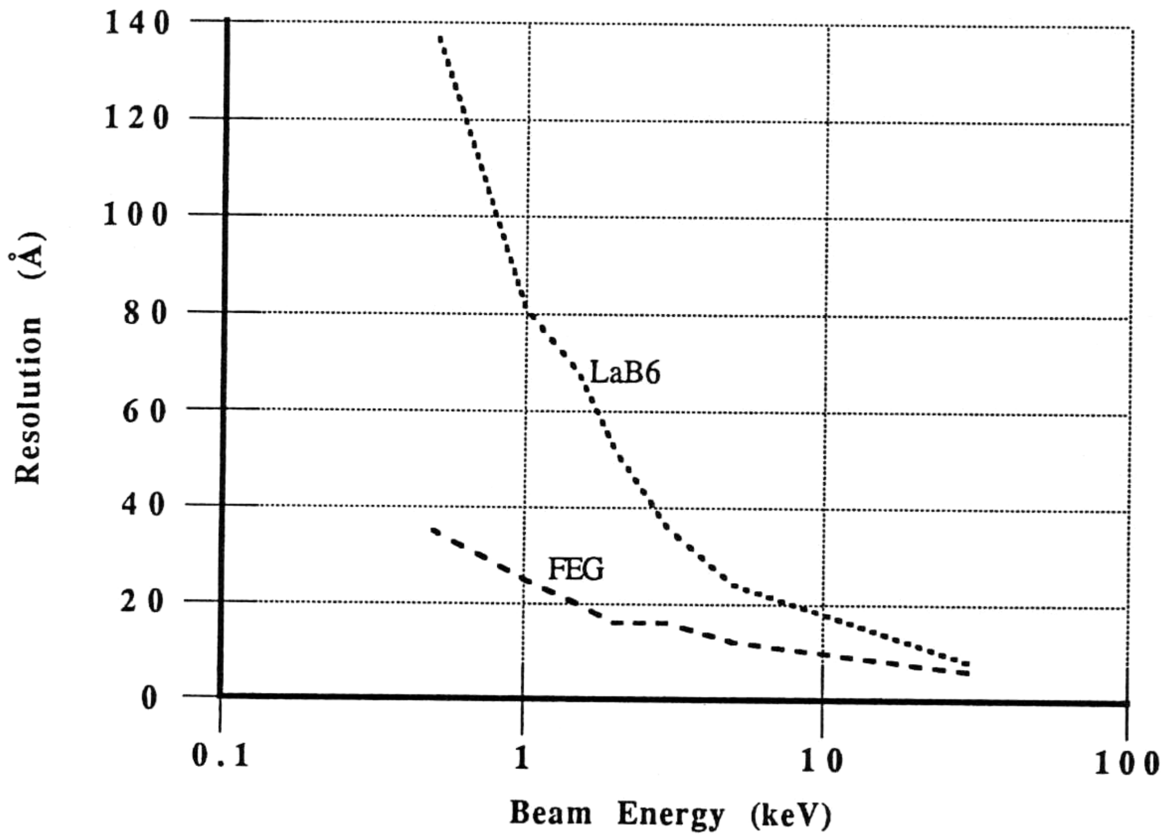

Fig. 6.- Resolution (10%-90% rise width) for FEG and LaB_6 emitters and the S-900 lens as a function of beam energy.

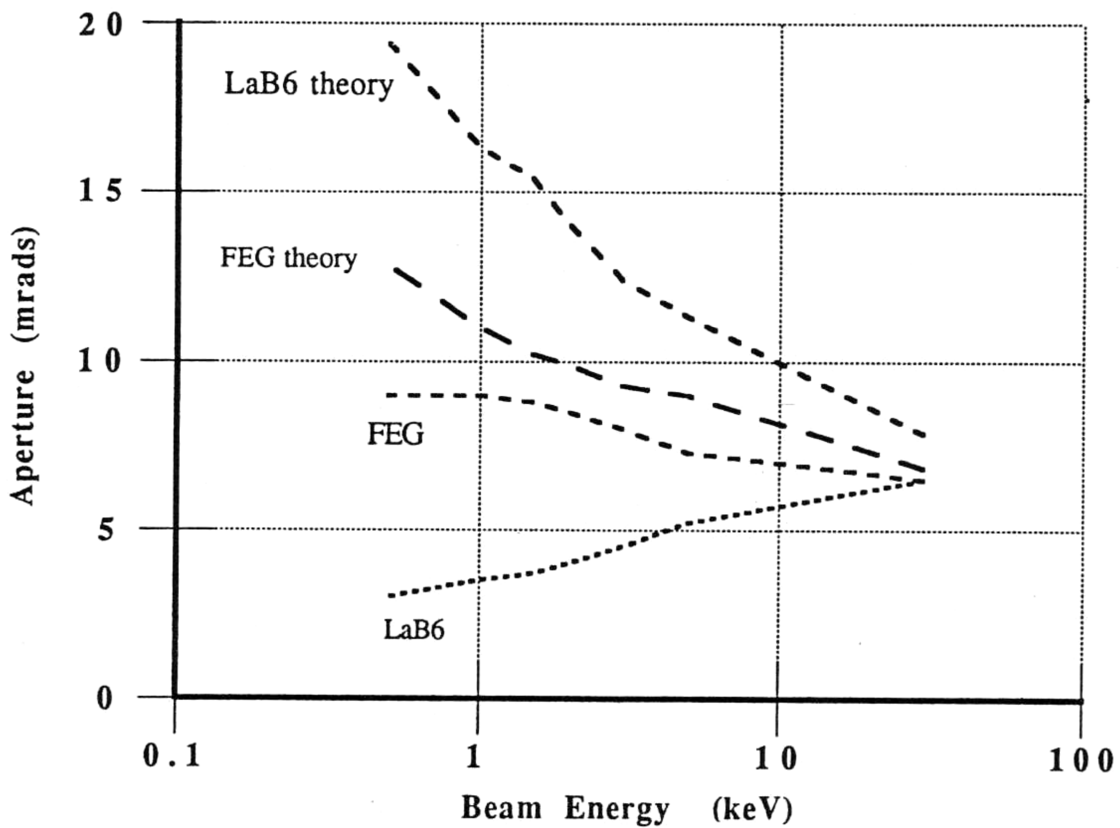

Fig. 7.- Optimum aperture for FEG and LaB_6 sources as a function of beam energy. The lines labeled 'Theory' show the corresponding aperture angles predicted by the simple analytical approach of equations (8) and (9).

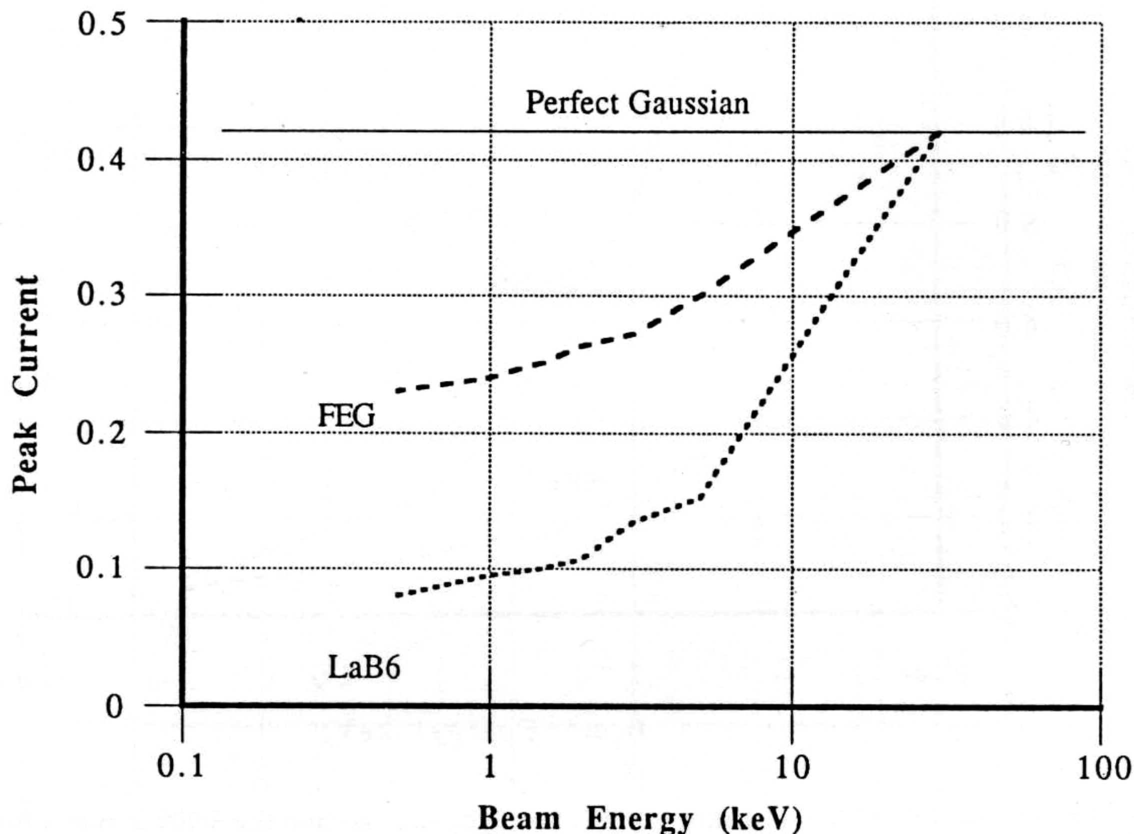

Fig. 8.- Variation of peak normalized axial current for FEG and LaB_6 sources demonstrating the trend away from Gaussian probe shape at low beam energies.

at high beam energies (>>10keV) the optimum beam aperture determined by this procedure differs in value from that predicated by simpler, less complete analyses. This is particulary true when termionic emitters of high energy spread are being used since it is chromatic aberration which leads to the rapid fall off in performance that is typical of low energy electron beam systems. The example worked in detail here was chosen to demonstrate that even with a state of the art probe forming lens the use of a field emission gun was still essential to obtain high performance. For less elaborate optics the penalty in performance is even more severe than that shown here.

A copy of the source code of this program, in Turbo Pascal, is available on request from the authors.

ACKNOWLEDGEMENTS

The authors are grateful to P.Kenway and G.Cliff for providing a copy of the original DOCCALC program, and to them and H.Darlington for valuable discussions. This work was partiatly supported by a grant from the IBM Corporation.

REFERENCES

1.- Kenway PB and Cliff G, (1984) Inst. Phys. Conf. Ser **68**,83.

2.- Lyman CE, Newbury DE, Goldstein JI, Williams DB, Romig AD, Armstrong JT, Echlin P, Fiori CE, Joy DC, Lifshin E, and Peters K-R, (1990) Scanning Electron Microscopy, X-ray Microanalysis and Analytical Electron Microscopy - A Laboratory Workbook, Plenum Press, New York.

3.- Smith KCA, (1972) Proc.5th SEM Symposium, ed O Johari, (IITRI: Chicago), 1.

4.- Joy DC, ,(1977) Proc. 10th SEM Symposium, ed O Johari, (IITRI: Chicago), 1.